Pergamon

Int. J. Multiphase Flow Vol. 20, No. 2, pp. 219–233, 1994

0301-9322/94 $7.00 + 0.00

FLOODING IN VERTICAL TUBES—I

EXPERIMENTAL STUDIES OF THE ENTRY REGION

C. E. LACY and A. E. DUKLER✠
Chemical Engineering Department, University of Houston, Houston, TX 77204, U.S.A.

(Received 20 April 1993; in revised form 16 September 1993)

Abstract—An experimental study of the liquid entry region during flooding is reported for a 50.8 mm i.d. vertical tube. The liquid entry device was a porous plastic tube into which film thickness measurement probes were mounted. Simultaneous measurements of the time-varying film thickness were made at locations below, inside and above the porous inlet. The weight of the evidence from cross-covariance analysis of these data does not appear to support models which assume upward propagation of waves above the feed point as the mechanism by which steady-state flooding takes place. Neither was there evidence that waves grow large enough to bridge the tube. Instead, the liquid film appears to undergo a transition from countercurrent to cocurrent flow inside the liquid feed. The pressure drop across the length of the porous tube was also measured and found to be significantly higher than that previously reported at locations above the liquid inlet. In part II [*Int. J. Multiphase Flow* **20**, 235–247 (1994)] a film model based on these data is explored.

Key Word: flooding, entry region, wire probes, porous inlet

INTRODUCTION

The flooding transition that occurs in falling-film systems has been the subject of numerous investigations for over 50 years. This interest in the transition has come from many areas, due to both the widespread application of gas–liquid flows and the undesirable effects that flooding can cause. In the process industries, for example, flooding can occur in many different unit operations, such as packed towers, falling-film chemical reactors and vertical tube condensers. Flooding in these situations results in an undesirable carryover of liquid. In the nuclear industry, a loss-of-coolant accident can create a flooding condition if the upward flow of steam limits the downward flow of emergency coolant to the reactor core, thereby increasing the possibility of meltdown.

To predict the onset of flooding, many empirical correlations have been suggested in the literature. Some examples are Wallis (1961), Clift *et al.* (1966), Tobilevich *et al.* (1968), Suzuki & Ueda (1977) and Ragland *et al.* (1989). A good comparison of these correlations and others can be found in McQuillan & Whalley (1985) and Bankoff & Lee (1986). Though many correlations now exist, each is limited to a narrow range of operating conditions, fluid properties, tube geometry and entry configurations similar to those on which the correlations were constructed. The reason for this limitation is that these correlations are not based on the physical mechanisms that cause flooding.

In an effort to develop better predictive models, many simple mechanisms have been presented in the published literature. Most of this work has focused on two models: (A) upward flow due to waves or (B) upward flow within the film.

(A) Wave models. Two mechanisms have been suggested for waves to cause flooding:

(1) Waves grow large enough to block the tube. The liquid in these waves is then accelerated upwards above the feed, either as a liquid slug or as a dispersed phase of entrained droplets. In this mechanism, flooding corresponds to the point of instability in the liquid film whereby waves can grow explosively. Some examples of models showing such instabilities can be found in the works by Shearer & Davidson (1965), Cetinbudaklar & Jameson (1969) and Zvirin *et al.* (1979).

✠Deceased February 1994.

(2) Waves propagate upward carring mass above the feed. As waves are seen to propagate downward below the flooding transition, flooding is assumed to occur when the gas flow is just sufficient for the waves to become stationary. Then, an incremental increase in the gas rate would cause these waves to flow upward above the feed to initiate flooding. Examples of this approach can be found in Ueda & Suzuki (1978) and McQuillan *et al.* (1985).

(B) Film models. In published models the existence of waves, their instability and growth are assumed to cause increasing interfacial shear stress and form drag. However, the flow field in the film is modeled by considering the mean film thickness subjected to this increased interfacial shear. Simplified models are then derived based on the steady-state solutions of a 1-D laminar film flow subjected to the interfacial shear stress resulting from the waves. Flooding occurs in these models when the interfacial shear is sufficient for one or more of these solutions to result in net upflow in the film. Examples of these approaches can be found in Solov'ev *et al.* (1967), Taitel *et al.* (1982) and Maron & Dukler (1984). In the latter, Maron & Dukler also develop models based on a flow-limiting kinematic wave and entrainment. As in the case of empirical correlations, none of these mechanisms has proved successful in predicting flooding over a wide range of operating conditions and tube geometry.

Laboratory studies of flooding have utilized two basic configurations of equipment. One consists of upper and lower tanks connected by a vertical tube, in which liquid flows downward by gravity from the top to the bottom tank. Gas is injected into the bottom tank and flows upward through the vertical tube to create counter current flow. Studies using this experimental configuration include those of Imura *et al.* (1977), Bharathan *et al.* (1978) and Liu *et al.* (1982). In the second configuration, liquid is injected as a film near the middle of the vertical tube through a porous section of pipe. Typically, this feed section consists of a porous sintered metal tube having small-diameter pores which produces an even distribution of liquid along the inner tube wall. With this configuration both flooding and flow reversal experiments can be conducted, and the distribution of the liquid between the upflow and downflow can be measured. This experimental arrangement has been used by many investigators, e.g. Hewitt & Wallis (1963), Suzuki & Ueda (1977), Kalb & Smith (1981), Zabaras & Dukler (1988) and Govan *et al.* (1991). Govan *et al.* have shown that even with a porous tube feed section, the gas and liquid rates at which flooding takes place can depend on the manner by which the gas and liquid are separated at the bottom of the tube.

In the Zabaras & Dukler (1988) study, detailed measurements of the instantaneous film thickness, pressure gradient and wall shear stress were obtained at different locations vertically below and far above the porous entry device. These data did not support either of the two wave-based mechanisms of flooding discussed above. Waves did not block the tube, and waves propagated downward just below the feed location. Furthermore, these studies indicated that the behaviors above and below the feed zone were completely uncoupled, a conclusion confirmed in the Govan *et al.* (1991) investigation. Since conditions at the feed were uncoupled from what takes place below the feed, Zabaras & Dukler (1988) suggested that flooding takes place when velocity distributions in the liquid film at the feed location change from uniformly downward to a split between upflow and downflow. Such a change in the velocity distribution takes place when, for any liquid rate, the interfacial shear stress there exceeds a critical value (Maron & Dukler 1984). *It is the objective of this study to explore that premise.*

In this paper (part I), the experimental results from simultaneous measurements of the time-varying film thickness inside the feed zone and the pressure gradient across the feed are reported. Additional film thickness measurements made at locations above and below the feed are also presented, along with the distribution of the liquid between the upflow and downflow. As will be shown, these data allow a more thorough investigation of wave motion as a possible flooding mechanism and provide detailed information to test film flow mechanisms. In part II (Lacy & Dukler 1994, this issue, pp. 235–247), the shape of the interface and the velocity distributions in the feed zone are computed. These are related to the interfacial shear by a direct numerical solution for the flow field using coordinate transformation methods to search for the free boundary shape. The computed shapes are then compared with the measurements reported in part I.

EXPERIMENTAL EQUIPMENT

Flow Loop

The flow loop for this study is shown in figure 1. The loop contained a 6.37 m long, vertical column consisting of sections of 50.8 mm i.d. acrylic tubing. The liquid was an aqueous NaCl solution (0.12 wt%) which entered at the feed measurement section as a film along the tube wall. Air entered at the bottom of the vertical column through a 1.59 m length of tube that served as a calming device for the air stream. In the bottom tank, the air contacted the liquid through a cone-shaped entrance which diverged the liquid film away from the upward flowing air stream, thus minimizing the interaction between the liquid and the air. The air then flowed up the vertical tube and was separated from the liquid film in the top tank using a similar cone-shaped exit device. Liquid in the form of entrained drops was then separated from the air stream, and the air vented to the atmosphere. The liquid in the film left the column through the top and bottom tanks by means of a level controller and control valve for each tank.

Measuring Stations and Techniques

The feed measurement section is shown in figure 2. A 114 mm long, porous plastic tube was mounted between two acrylic tubes with the porous tube's outer surface surrounded by a liquid-filled reservoir. The porous tube was carefully machined to 50.8 mm i.d. to match the acrylic

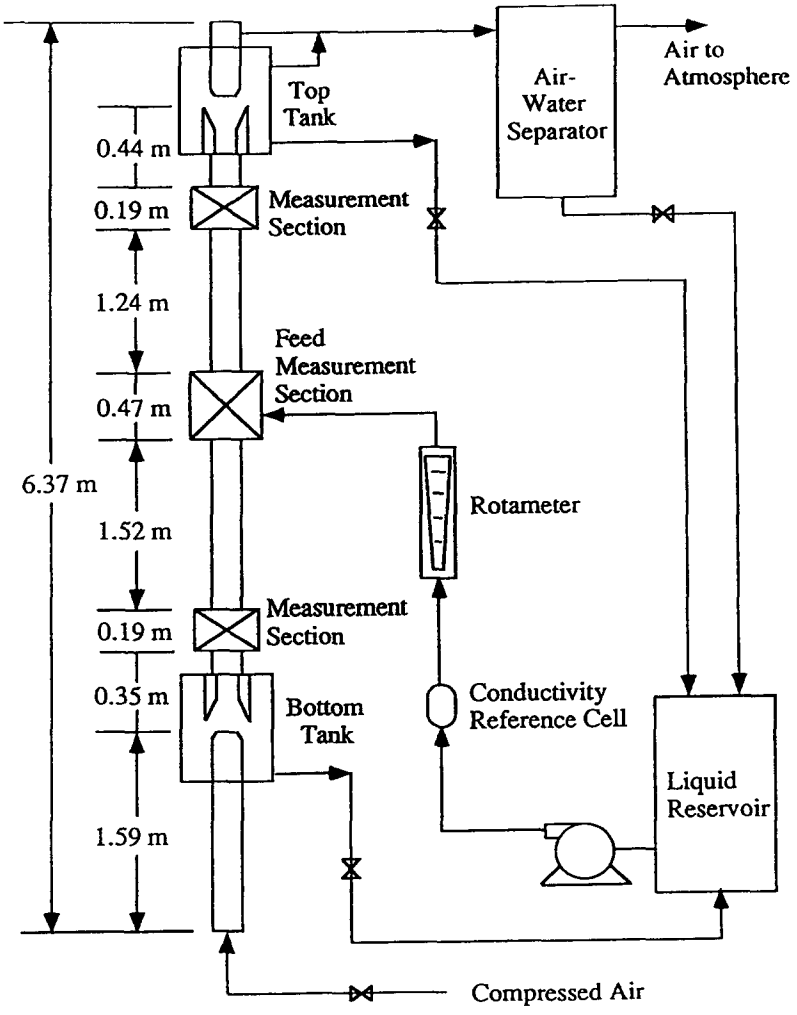

Figure 1. Schematic of the flow loop.

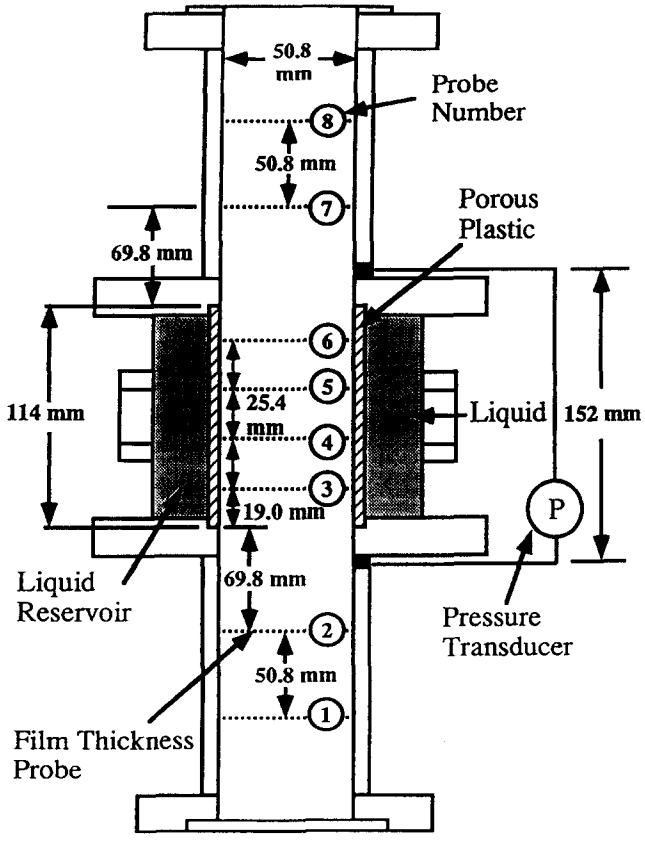

Figure 2. Feed measurement section.

tubes, in order to minimize any disturbances to the liquid flow. A variable-reluctance differential pressure transducer was used to measure the time-varying pressure gradient across the feed over a distance of 152 mm. To measure the film thickness, the section contained 8 film thickness probes—numbered 1–8 in figure 2—consisting of two parallel platinum–13% rhodium wires, 75 μm o.d. In the porous tube, 4 probes (numbered 3–6) were mounted, as shown in figure 3, with a vertical spacing of 25.4 mm between the probes. Two additional probes were mounted on each side of the feed (numbered 1 and 2 below and 7 and 8 above) with a vertical spacing of 50.8 mm. The two other measurement sections shown in figure 1 were identical in construction and contained two film thickness probes also with a vertical spacing of 50.8 mm. Except for probes 3–6, these film thickness probes were similar in construction to that of Zarabas *et al.* (1986). All probes were calibrated using the Taylor-bubble technique recently developed by Bousman *et al.* (1994).

To measure the time-varying film thickness, new electronic circuitry had to be developed so that simultaneous, yet independent, measurements could be obtained for all 12 probes. Figure 4 shows a conceptual schematic of the circuitry used in this study. The design incorporates the suggestion by Brown *et al.* (1978) that only one channel be activated at any given instant, to prevent crosstalk between adjacent ground connections. The circuit differs, however, from those reported in the past (e.g Zabaras *et al.* 1986; Koskie *et al.* 1989), as there is no sine-wave carrier frequency which must be demodulated. Instead, a single, very short duration square wave is applied to a probe for the time interval of each measurement and a reading taken after the transient has decayed. This circuit proved to be extremely linear with conductance and produced no measurable interaction between the probes.

Operating Conditions

Experimental data were collected for five liquid feed rates corresponding to $Re_F = 4\Gamma/\nu = 300$ to 3000, where Γ is the liquid downflow rate per unit perimeter and ν is the kinematic viscosity.

The gas flowrate was either zero (free-falling film) or varied from $Re_G = 15{,}000$ to 50,000. For a given liquid and gas flowrate after flooding, simultaneous measurements of the 12 film thickness probes and the pressure gradient were recorded for 135 s. Below the flooding point, only the 8 film thickness probes located inside and below the feed were measured. All data were digitized at 1000 Hz using a 12-bit A/D converter on a microcomputer. Further details of the equipment, experimental techniques, and a complete tabulation of experimental data are given by Lacy (1992).

MEASUREMENTS

Liquid Distribution

Before the flooding point, all of the injected liquid flows downward as a liquid film. Once flooding occurs, part of this liquid flows upwards. Figure 5 shows a comparison of the experimental liquid downflow rates obtained in this study with those of Zabaras & Dukler (1988) and Dukler & Smith (1979). For each increase in the gas flowrate after flooding, the liquid downflow rate decreases. The shape of this curve is independent of the liquid injection rate. The two previous studies shown in figure 5 used sintered metal tubes, while in this study a porous plastic tube was used. These 3 tubes have different vertical lengths and pore sizes. Therefore, the close agreement between the downflow rates shows that detailed characteristics of the porous section have little effect.

Film Thickness Time Trace

Typical traces of the time-varying film thickness just after flooding are shown in figure 6 for $Re_F = 1500$ and $Re_G = 34{,}700$. These data were taken at various positions below, inside and above the feed. Given such data, some of the questions that must be addressed are:

(1) What changes occur in the liquid film inside the feed? Do these changes suggest that the feed is a transition region between countercurrent and cocurrent flow or is the film inside the feed quite different from the film thickness measured both below and above the feed?

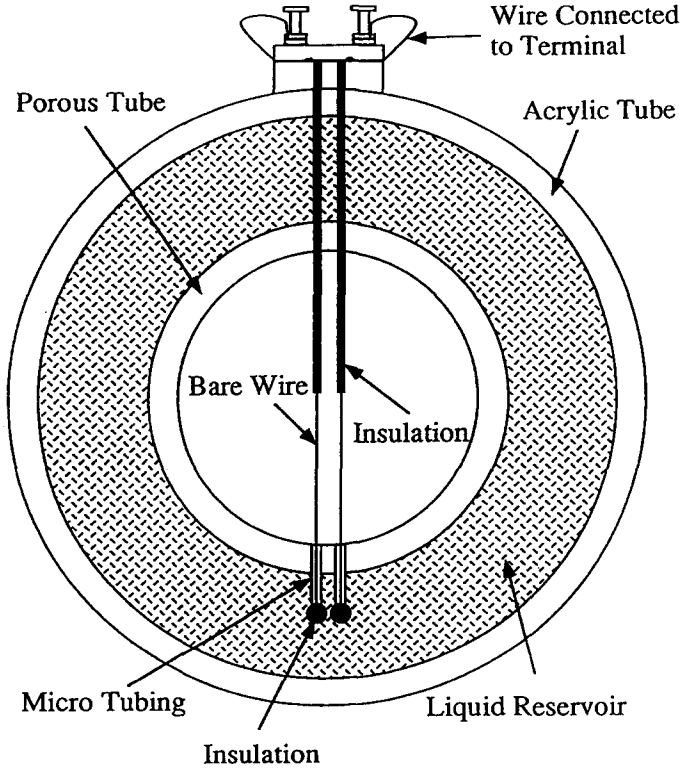

Figure 3. Film thickness probes inside the feed.

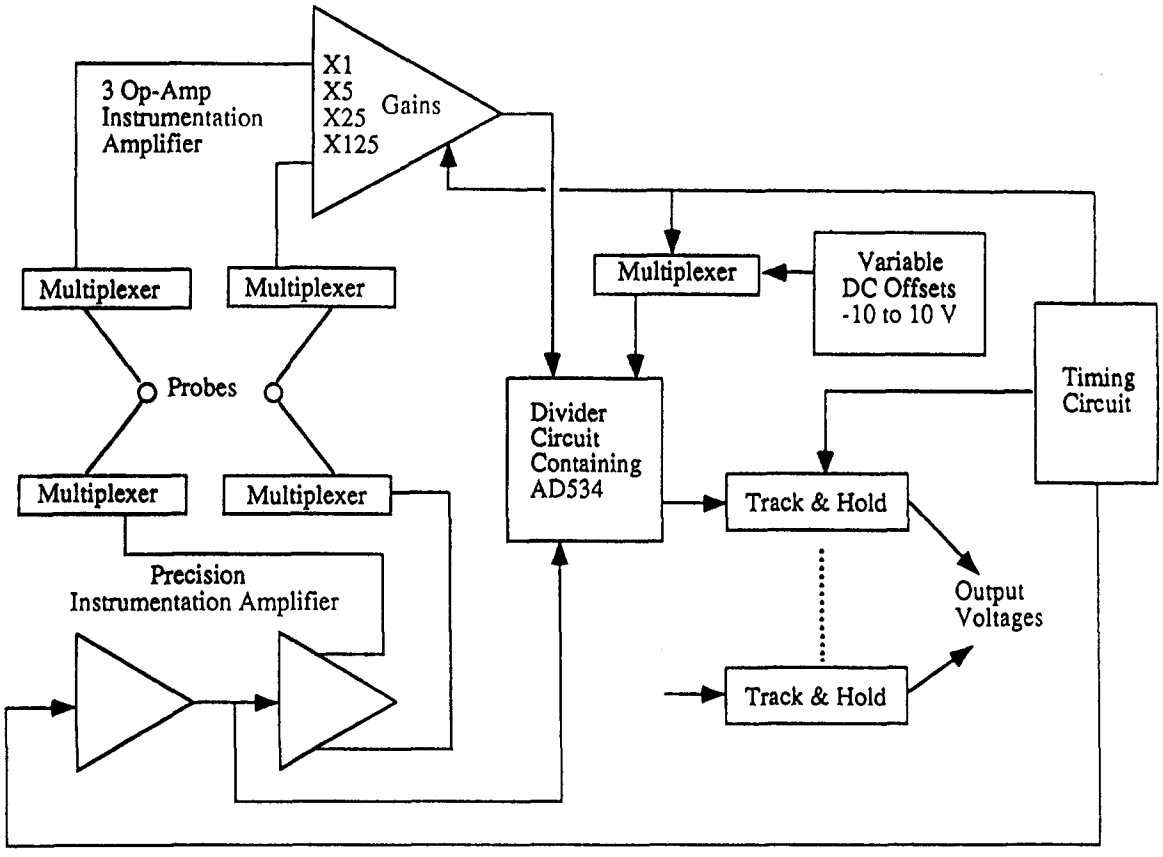

Figure 4. Film thickness monitoring circuitry.

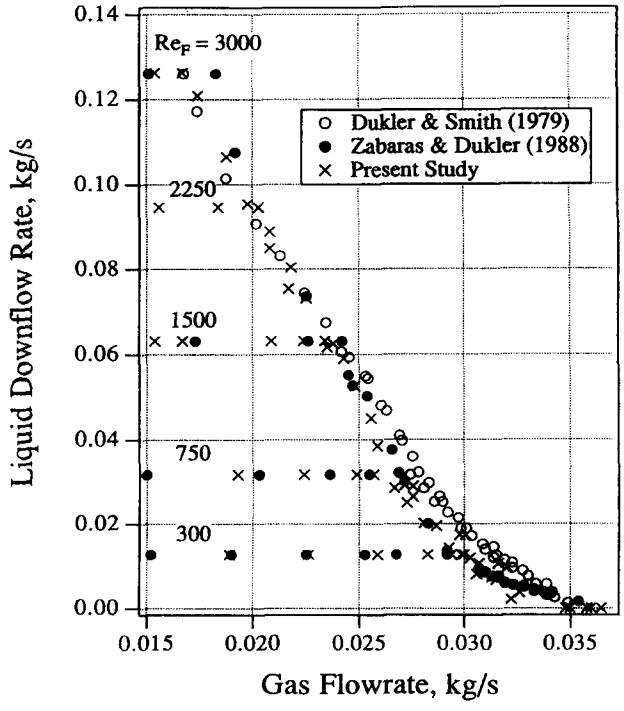

Figure 5. Liquid downflow rate.

(2) Do the large film thickness peaks shown in figure 6 often approach the radius of the tube, i.e. do waves grow large enough to block the gas flow to cause flooding?
(3) Do these waves propagate upward, thus carrying mass above the feed to cause flooding? Or do the waves propagate at all inside the feed?

These questions and others will be addressed in the analysis that follows.

Mean Film Thickness

Figure 7 shows the mean film thicknesses for probes 1–8 at flooding as a function of the vertical distance from probe 1 (see figure 2). Data are shown for each liquid feed rate at the lowest gas flowrate in which cocurrent gas–liquid flow could be established above the feed. In general, these data show that the mean film thickness increases monotonically from below the feed (probe 1) to above the feed (probe 8). Probes 3–6 inside the feed thus appear to be a transition between countercurrent flow below the feed and cocurrent flow above the feed. When the feed splits between

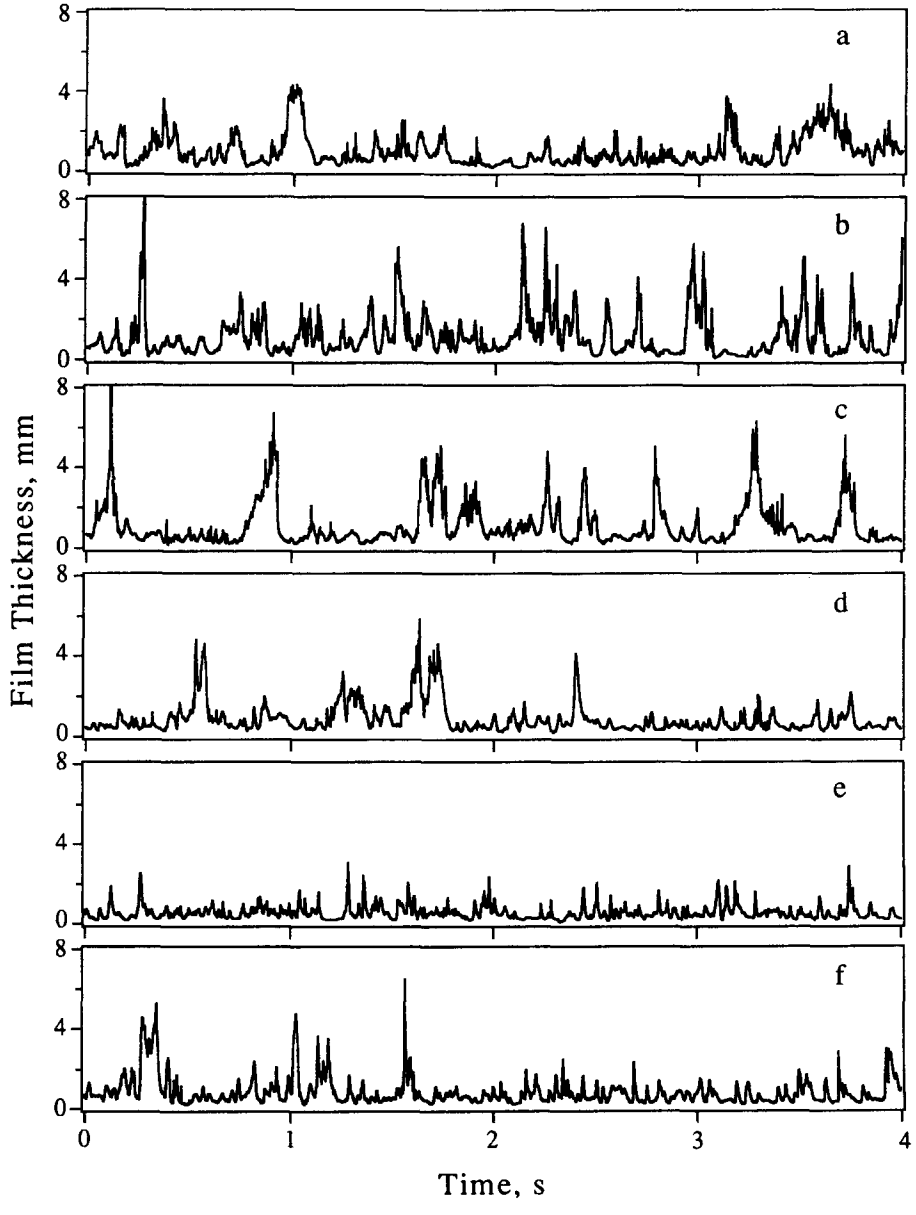

Figure 6. Film thickness traces for $Re_F = 1500$, $Re_G = 34{,}700$ and 17% upflow.

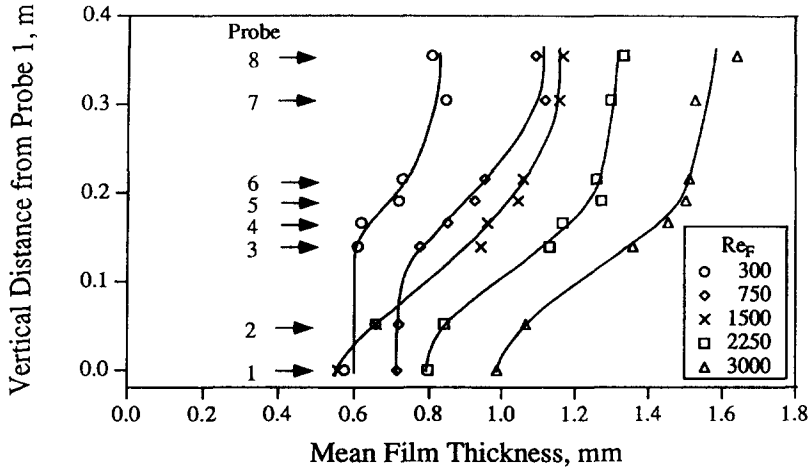

Figure 7. Film thickness profiles across the feed at flooding.

the upward and downward flow for a given liquid feed rate, the qualitative picture remains the same, as shown in figure 8 for $Re_F = 3000$.

Figure 7 shows that for $Re_F = 1500$ the film thickness at the lowest probe is smaller than for $Re_F = 300$ and 750. This is not an anomaly in the data, as can be seen by a study of figure 9. Note from figure 9 that at probe 2 the film thickness along the flooding curve is not monotonic. The film thickness at flooding decreases with decreasing liquid feed rate until $Re_F \approx 1000$, where it reaches a local minimum and then a maximum after which it continues its decreasing trend. The process of flooding can be considered the first transition and this abrupt change in the film thickness curve at flooding is designated as the second transition. As a result of the second transition, the film thickness at flooding for $Re_F = 300$ is larger than that at $Re_F = 1500$, thus confirming the accuracy of the film thickness profile in figure 7. This transition coincides with a change in wave structure of the liquid film, which was visually apparent and which is indicated by the

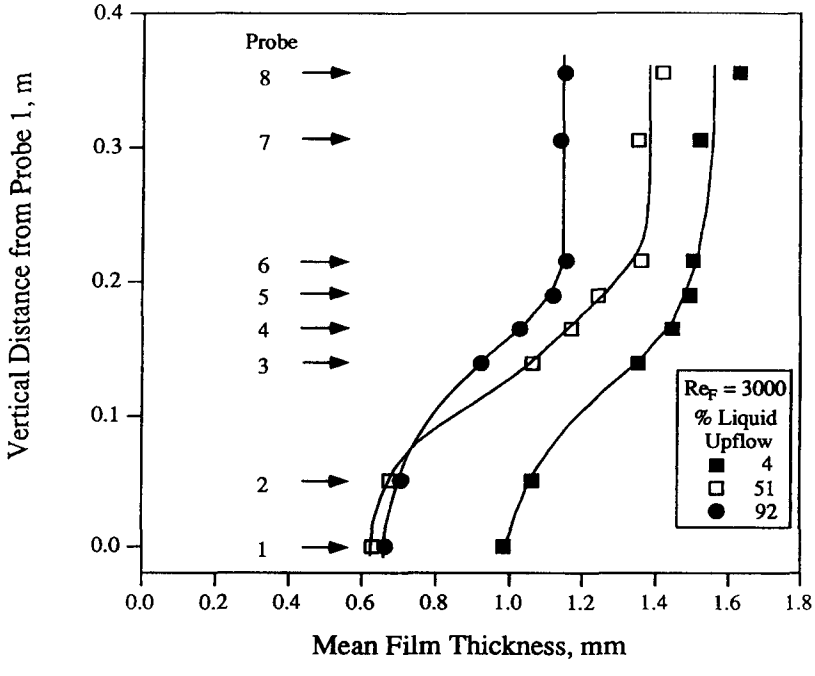

Figure 8. Film thickness profiles at $Re_F = 3000$ as a function of the liquid upflow rate: Re_G at 4% = 24,400, at 51% = 33,300, at 92% = 45,000.

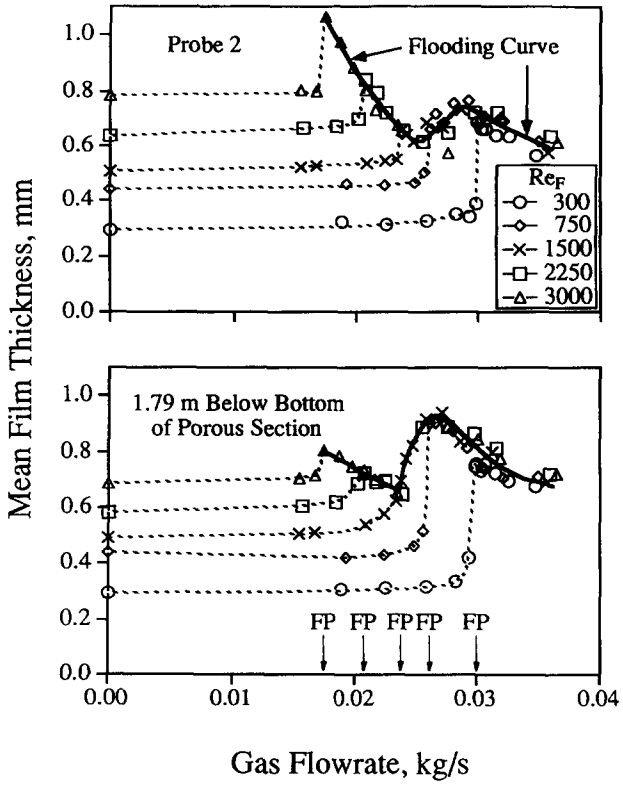

Figure 9. Mean film thickness below the porous section.

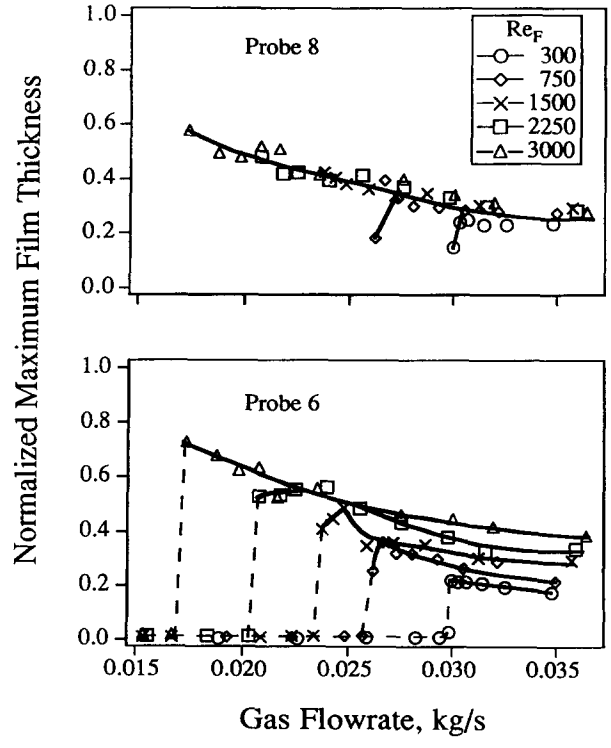

Figure 10. Maximum film thickness.

cross-covariance data presented below. Govan *et al.* (1991) also reported such a second transition when using a cone-shaped exit similar to that used in this study. They suggested that the second transition was due to flooding being initiated at the liquid exit, however, that did not appear to be the case in these studies. The analysis which follows will show that the changes observed near the liquid exit also take place within the feed zone itself.

Maximum Film Thickness

To test whether large waves frequently block the tube to cause flooding, the maximum film thickness must be considered. Figure 10 shows the maximum film thickness normalized by the tube radius for probes 6 and 8. These probes displayed the largest maximum film thicknesses of any of the 12 probes in the test section. Each point in figure 10 represents the average of the 10 largest waves obtained during a 135-s time trace. For bridging to be a feasible mechanism for flooding, one would expect the film thickness to repeatedly approach the radius of the tube so that the maximum film thickness would be approx. 1. In no case, however, did repeated bridging of the tube occur in this study. Only for $Re_F = 3000$ does the maximum film thickness exceed 60% of the tube radius. In most cases the maximum film thickness was $\leqslant 50\%$ of the radius. It must be remembered that this maximum thickness corresponds to the largest peaks which occur, on average, only once every 10–15 s. Data taken at the other 10 film thickness probes showed similar results. Thus, no evidence was found at any position in the vertical column to support the bridging mechanism.

Cross-covariance Analysis

Cross-covariance studies were carried out between the 8 probe pairs mounted in the measuring station, as well as between probes located above and below the feed. Typical results from probes located 1.79 m below the bottom of the porous section for 5 feed rates and measured just at flooding are shown in figure 11. A peak at a positive time delay corresponds to upward wave propagation, while one at a negative time delay indicates downward propagation. The existence of well-defined downward wave velocities is clearly evident for $Re_F \geqslant 1500$. But the small peaks which appear at $Re_F = 300$ and 750 are within the standard error for the data, as computed by the method of Bendat & Pearsol (1986). Therefore, there appears to be a change in the wave structure such that wave propagation is suppressed for lower Re_F values. This takes place at $Re_F \approx 1000$, at which the second transition in film thickness occurs (as discussed above). Exactly the same transition also takes place within the feed zone. Figure 12 shows the cross-covariance of the film thickness as measured

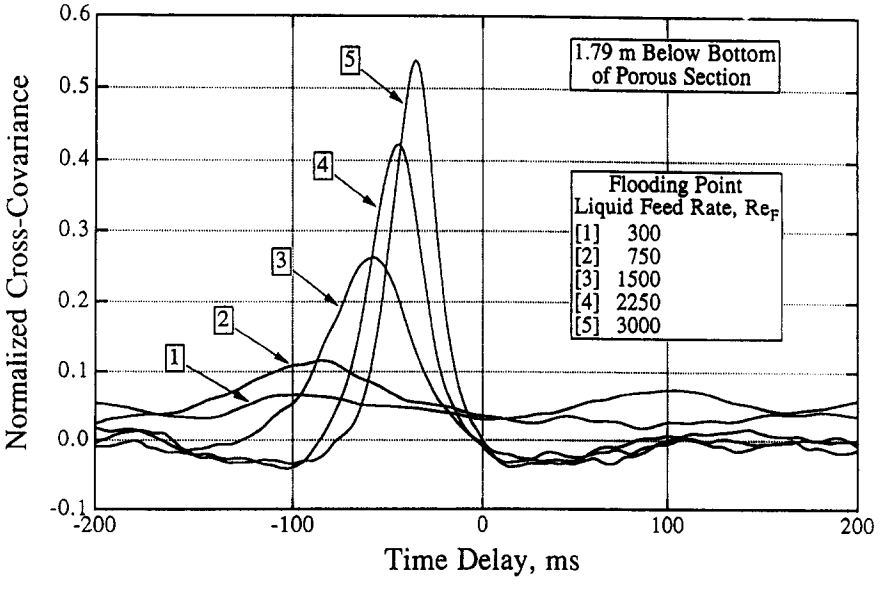

Figure 11. Cross-covariance at flooding 1.79 m below the bottom of the porous section.

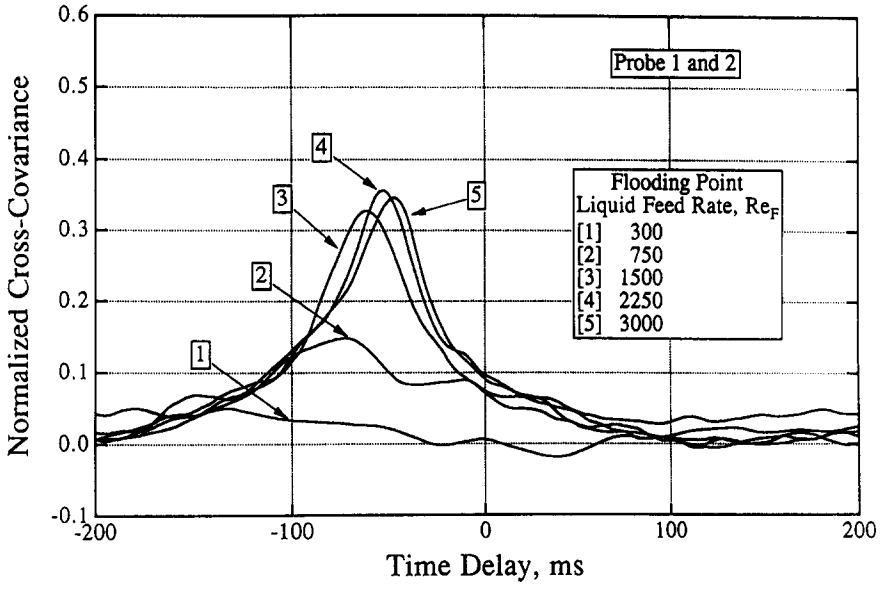

Figure 12. Cross-covariance at flooding for probes 1 and 2.

between probes 1 and 2 within the feed section. Downward propagating waves are present at $Re_F > 1000$ but can no longer be discerned at $Re_F < \sim 1000$. Thus, it is clear that this transition does not take place only at the tube exit as suggested by Govan *et al.* (1991). It takes place everywhere below the feed at almost the same gas flowrates.

Further evidence can be offered to show that liquid carried by waves from below to above the feed is not the mechanism for flooding. Consider figure 13, which shows the cross-covariance of the film thickness taken at probes 3 and 4 which are located in the lower part of the porous tube. At $Re_F > 1000$ the direction of wave propagation is downward. At lower feed rates there is no discernible wave propagation in either direction. The very small positive peaks at $Re_F = 300$ and 750 are within standard error bounds. Similarly the cross-covariance between probes 5 and 6, located at the top of the porous tube, shows no evidence of upward wave propagation (as indicated in figure 14). The existence of both positive and negative peaks suggests the existence of an oscillatory motion of the waves. Thus, the weight of the experimental evidence seems to suggest

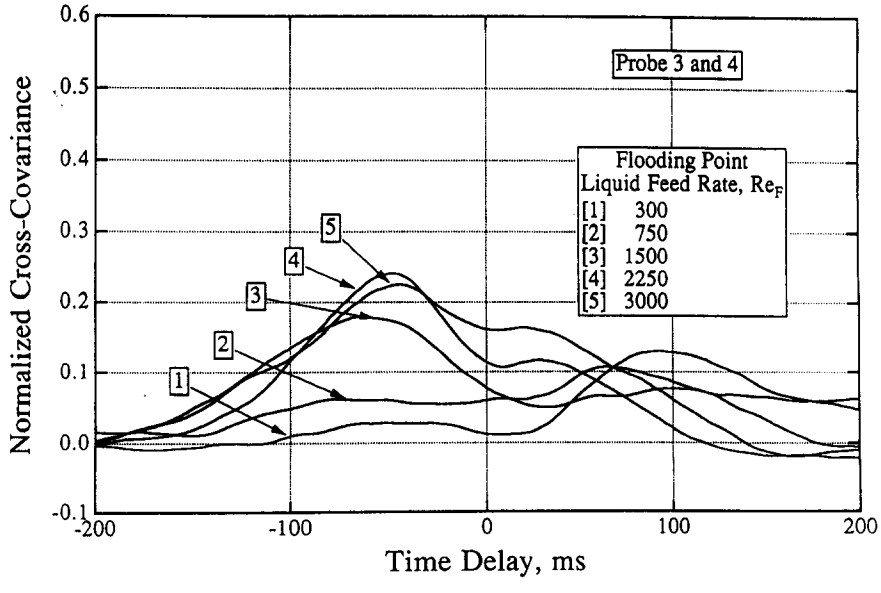

Figure 13. Cross-covariance at flooding for probes 3 and 4.

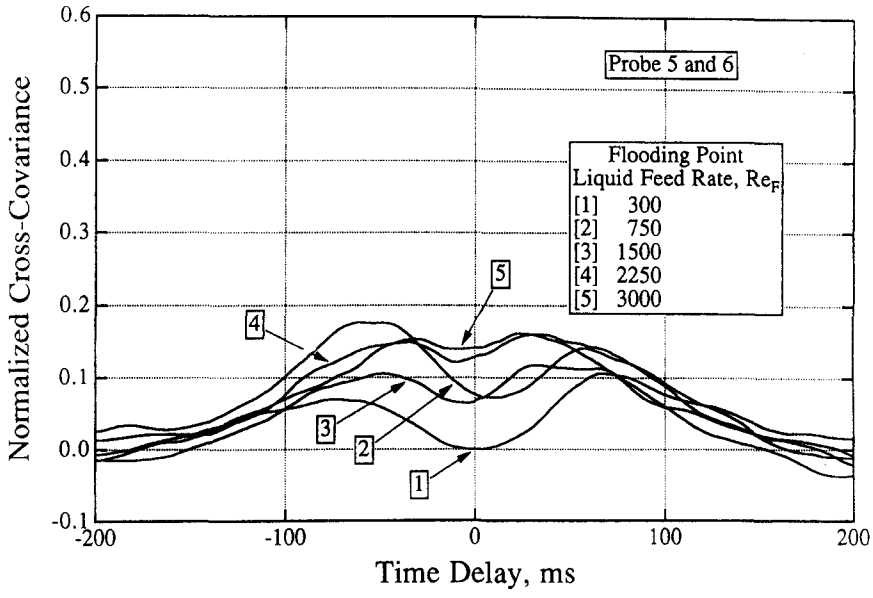

Figure 14. Cross-covariance at flooding for probes 5 and 6.

that the mechanism of flooding does not involve a reversal in the direction of the waves such that they carry liquid above the feed. Rather it is hypothesized that the upward flow results from a shift in the velocity profile within the film at the feed location.

Power Spectra

The normalized power spectra of the film thickness at flooding are presented in figure 15. Data are shown for 4 different positions along the vertical column for $Re_F = 750$ and 3000. The spectral

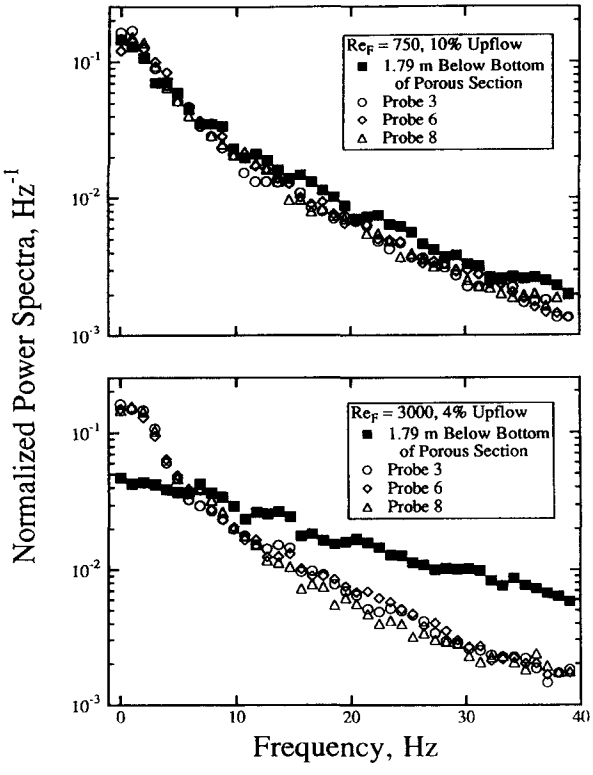

Figure 15. Normalized power spectra at flooding.

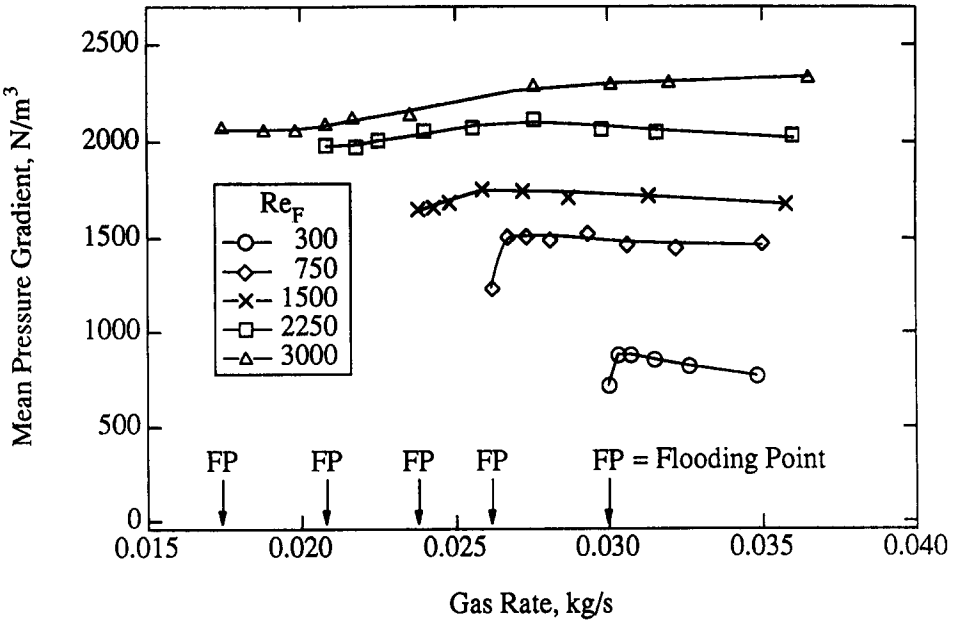

Figure 16. Mean pressure gradient across the feed.

character of the waves *inside and above* the feed are quite similar at flooding for both of these conditions. At $Re_F = 750$, a liquid feed rate less than that for the second transition, the waves on the film *below the feed* are similar in spectrum to those at the other locations. In contrast, for feed rates greater than that at the second transition, say at $Re_F = 3000$, the power spectrum *below the feed* is quite different from those *inside and above the feed.* Since both the spectra and the cross-covariance are similar at all points in the column after the second transition, it is probable that the same mechanism that causes flooding also causes this transition.

Pressure Gradient

The mean pressure gradient across the feed region (see figure 2) is shown in figure 16. Experimental data were collected for all conditions where a liquid film existed at both pressure taps. From these data, it would appear that changes in the upflow rate have little effect on the mean pressure gradient. Dukler *et al.* (1984) used an almost identical configuration to that in figure 1 and measured the average pressure gradient above the feed taken over a distance of 1.78 m. Comparison of the data from this study with that of Dukler *et al.* showed that the pressure gradient inside the feed zone is about 50% larger than that above the feed under similar conditions. This suggests that a higher interfacial shear stress is needed to distribute the liquid as it enters the tube through the porous wall.

SUMMARY

Experimental evidence is presented using a porous tube feed system which suggests that the wave basis for explaining flooding is invalid. That is, wave growth and blocking of the tube or wave propagation along the film from below to above the feed does not take place. Instead a mechanism is suggested, whereby the velocity distribution changes direction in the film in the vicinity of the porous tube feed zone such that some of the liquid in the film flows upward. Measurements of the film thickness profile and pressure gradient within this feed zone are reported.

REFERENCES

BANKOFF, S. G. & LEE, S. C. 1986 A critical review of the flooding literature. In *Multiphase Science and Technology*, Chap. 2 (Edited by HEWITT, G. F., DELHAYE, J. M. & ZUBER, N.) pp. 95–180. Hemisphere, New York.

BENDAT, J. S. & PEARSAL, A. G. 1986 *Random Data*, 2nd edn. Wiley, New York.

BHARATHAN, D., WALLIS, G. B. & RICHTER, H. J. 1978 Air–water countercurrent annular flow in vertical tubes. Electric Power Research Institute Report EPRI NP-786.

BOUSMAN, W. S., JANICOT, A. & DUKLER, A. E. 1994 Film thickness calibration of two wire conductance probes in small diameter tubes. Unpublished manuscript.

BROWN, R. C., ANDREUSSI, P. & ZANELLI, S. 1978 The use of wire probes for the measurement of liquid film thickness in annular gas–liquid flows. *Can. J. Chem. Engng* **56,** 754–757.

CETINBUDAKLAR, A. G. & JAMESON, G. J. 1969 The mechanism of flooding in vertical countercurrent two-phase flow. *Chem. Engng Sci.* **24,** 1669–1680.

CLIFT, R., PRITCHARD, C. L. & NEDDERMAN, R. M. 1966 The effect of viscosity on the flooding conditions in wetted wall columns. *Chem. Engng Sci.* **21,** 87–95.

DUKLER, A. E. & SMITH, L. 1979 Two phase interactions in countercurrent flow: studies of the flooding mechanism. U.S. Nuclear Regulatory Commission Report NUREG/CR-0617.

DUKLER, A. E., SMITH, L. & CHOPRA, A. 1984 Flooding and upward film flow in tubes—I: experimental studies. *Int. J. Multiphase Flow* **10,** 585–597.

GOVAN, A. H., HEWITT, G. F., RICHTER, H. J. & SCOTT, A. 1991 Flooding and churn flow in vertical pipes. *Int. J. Multiphase Flow* **17,** 27–44.

HEWITT, G. F. & WALLIS, G. B. 1963 Flooding and associated phenomena in falling film flow in a vertical tube. UKAEA Report AERE-R4022.

IMURA, H., KUSUDA, H. & FUNATSU, S. 1977 Flooding velocity in a counter-current annular two-phase flow. *Chem. Engng Sci.* **32,** 79–87.

KALB, C. E. & SMITH, J. K. 1981 An interpolative flooding model based on limiting flow regimes for countercurrent gas/liquid flow. *Chem. Engng J.* **18,** 113–123.

KOSKIE, J. E., MUDAWAR, I. & TIEDERMAN, W. G. 1989 Parallel-wire probes for measurement of thick liquid films. *Int. J. Multiphase Flow* **15,** 521–530.

LACY, C. E. 1992 Flooding and wavy films in vertical annular gas–liquid flows. Ph.D. Dissertation, Univ. of Houston, Houston, TX.

LACY, C. E. & DUKLER, A. E. 1994 Flooding in vertical tubes—II. A film model for entry region flooding. *Int. J. Multiphase Flow* **20,** 235–247.

LIU, P., MCCARTHY, G. E. & TIEN, C. L. 1982 Flooding in vertical gas–liquid countercurrent flow through multiple short paths. *Int. J. Heat Mass Transfer* **25,** 1301–1312.

MARON, D. M. & DUKLER, A. E. 1984 Flooding and upward film flow in vertical tubes—II: speculations on film flow mechanisms. *Int. J. Multiphase Flow* **10,** 599–621.

MCQUILLAN, K. W. & WHALLEY, P. B. 1985 A comparison between flooding correlations and experimental flooding data for gas–liquid flow in vertical circular tubes. *Chem. Engng Sci.* **40,** 1425–1440.

MCQUILLAN, K. W., WHALLEY, P. B. & HEWITT, G. F. 1985 Flooding in vertical two-phase flow. *Int. J. Multiphase Flow* **11,** 741–760.

RAGLAND, W. A., FRANCE, D. M. & MINKOWYCZ, W. J. 1989 Two-phase flow at the flooding point in an annulus. *Expl Therm. Fluid Sci.* **2,** 7–16.

SHEARER, C. J. & DAVIDSON, J. F. 1965 The investigation of a standing wave due to gas blowing upwards over a liquid film; its relation to flooding in wetted-wall columns. *J. Fluid Mech.* **22,** 321–335.

SOLOV'EV, A. V., PREOBRAZHENSKII, E. I. & SEMENOV, P. A. 1967 Hydraulic resistance in two-phase flow. *Int. Chem. Engr* **7,** 59–63.

SUZUKI, S. & UEDA, T. 1977 Behaviour of liquid films and flooding in counter-current two-phase flow. Part I. Flow in circular tubes. *Int. J. Multiphase Flow* **3,** 517–532.

TAITEL, Y., BARNEA, D. & DUKLER, A. E. 1982 A film model for the prediction of flooding and flow reversal for gas–liquid flow in vertical tubes. *Int. J. Multiphase Flow* **8,** 1–10.

TOBILEVICH, N. Y., SAGAN', I. I. & PORZHEZINSKII, Y. G. 1968 The downward motion of a liquid film in vertical tubes in an air–vapor counterflow. *J. Engng Phys.* **15,** 1071–1076.

UEDA, T. & SUZUKI, S. 1978 Behaviour of liquid films and flooding in counter-current two-phase flow. Part 2. Flow in annuli and rod bundles. *Int. J. Multiphase Flow* **4,** 157–170.

WALLIS, G. B. 1961 Flooding velocities for air and water in vertical tubes. UKAEA Report AEEW-R1213.

ZABARAS, G. J. & DUKLER, A. E. 1988 Countercurrent gas–liquyid annular flow, including the flooding state. *AIChE Jl* **34,** 389–396.

ZABARAS, G. J., MARON, D. M. & DUKLER, A. E. 1986 Vertical upward cocurrent gas–liquid annular flow. *AIChE Jl* **32,** 829–843.

ZVIRIN, Y., DUFFEY, R. B. & SUN, K. H. 1979 On the derivation of a countercurrent flooding theory. In *Proc. Symp. on Fluid Flow and Heat Transfer over Rod or Tube Bundles*, pp. 111–119. ASME, New York.